PRACTICAL APPLICATIONS OF HYPERSPECTRAL REMOTE SENSING IN REGOLITH RESEARCH

Ian C. Lau[1], Tom J. Cudahy[2], Graham Heinson[1], Alan J. Mauger[3] & Patrick R. James[1].

[1]CRC LEME, School of Earth and Environmental Science, University of Adelaide, Adelaide, SA, 5005
[2]Mineral Mapping Technologies Group, CSIRO Exploration & Mining, PO Box 1130, Bentley, WA, 6102
[3]PIRSA, Office of Minerals and Energy Resources, GPO Box 1671, Adelaide, SA, 5001

INTRODUCTION

Hyperspectral data consist of many measurements of discrete spectral wavelengths (typically >100) across the electromagnetic spectrum within the atmospheric transmission windows. Examples of hyperspectral sensors in operation in Australia are HyVista's HyMap™ (http://www.hyvista.com/), the Compact Airborne Spectrographic Imager (CASI) and De Beers' Airborne Multispectral Scanner (AMS). The HyMap™ airborne scanner consists of 128 bands covering the region between 400 and 2500 nanometres (nm) (Cocks *et al.* 1998). This region consists of visible, near infrared (VNIR) and shortwave infrared (SWIR) wavelengths. This wavelength region contains diagnostic absorptions of iron oxide, phyllo-silicate, and carbonate minerals, as well as vegetation components such as chlorophyll, starch, waxes, lignin and cellulose (Lewis *et al.* 2001). Airborne hyperspectral imagery (AHSI) must be corrected to remove the effects of the atmosphere before results comparable to laboratory spectrometers can be obtained. Spectrometers used in the laboratory and the field, such as the Geophysical Environmental Research Inc (GER) IRIS, Analytical Spectral Devices Inc (ASD) FieldSpec Pro FR or Integrated Spectronics Pty Ltd Portable Infrared Mineral Analyser (PIMA) (SWIR only), generally possess more spectral bands (potentially better spectral resolution) than remote sensing systems, allowing the resolution of closely spaced absorptions from different minerals. Laboratory measurements using a halogen light source permit the recording of spectral responses of minerals without atmospheric effects. Measurement of geological samples with a field/laboratory instrument also avoids problems with trying to "un-mix" vegetation effects which often beset processing of AHSI data.

Hyperspectral airborne surveys encounter limitations similar to airborne gamma-ray spectroscopy surveys in that they examine the materials occurring at the very surface, which may or may not be similar to the underlying regolith. An opportunity to observe the regolith stratigraphy arises where incised landscapes expose formerly "covered" materials, which enables remote sensing data to provide more accurate maps of the regolith landform units. Field measurements of samples from exploration trenches and drill core provides an alternate means of understanding regolith stratigraphy, which can also be used to better interpret the information displayed by the airborne data, as well as improve the understanding of the mineralogy of the regolith. The following research demonstrates the practical uses of hyperspectral airborne imagery and laboratory spectral sampling in regolith geoscience.

WHITE DAM PROSPECT

The White Dam Cu-Au prospect is located in the Curnamona Province of South Australia, approximately 30 km NE of Olary. An Au anomaly was identified by regional soil sampling and was followed-up by drilling in the late 1990s. The mineralisation occurs under a cover of approximately 1 m thick aeolian, colluvial and alluvial sands with minor mineralisation occurring at approximately 45 m (McGeough & Anderson 1998). Recent costeans dug across the interpreted mineralised area excavated a maximum of two metres of transported material before intersecting saprolite. The depth to weathered bedrock increased from less than 0.5 m to 2 m at the northern end of the costeans as they pass from an erosional rise of slightly weathered quartzo-felspathic biotite gneiss into a flanking drainage line.

SAMPLING AND SPECTRAL ANALYSIS

Seventy soil and eighty eight bladder saltbush (*Atriplex vesicaria*) samples were collected from surface traverses over the prospect for geochemical and biogeochemical analyses. Thirty two profiles were sampled from five costeans at 10 m spacings. The profile samples were collected at 0.25 m intervals to a depth of 5.5 m. The profiles sampled a number of horizons of transported and *in situ* material into weathered bedrock. The seventy surface and six hundred profile samples were measured by an ASD FieldSpec Pro FR spectrometer to ascertain if their mineralogy could be determined by spectral methods alone. Powdered samples placed on a glass petri dish were then placed on the vertically mounted High-Intensity Contact Probe, which housed a 100 W halogen lamp and an aperture for the fibre-optic cable (Figure 1). A series of measurements were taken of the different morphologies for each sample. Quantitative X-ray diffraction (XRD) analysis was performed on a profile and specific samples to test the validity of minerals identified by

In: Roach I.C. ed. 2003. *Advances in Regolith*, pp. 249-253. CRC LEME.

the spectral method and to aid in the modelling of quantitative abundances of regolith materials.

HYPERSPECTRAL DATA

Five NE trending swaths of HyMap™ imagery were acquired over the White Dam Prospect in November 1998 at a 5 m ground resolution. A combination of HYCORR software, which creates a model of the atmosphere, and an empirical line technique were used to correct the most coherent swath. The neighbouring runs were normalised using the gains generated in the above correction process. An ASD FieldSpec measurement of a suitable bright target was deconvoluted to match HyMap™ spectral bands and used as the calibration spectra in the empirical line and normalisation techniques.

RESULTS AND DISCUSSION

The ASD spectra of the surface soil samples showed little variation with a persistent spectral signature from surficial materials showing a symmetrical absorption feature at 2207 nm related to Al-OH (Figure 2). An inflection in the reflectance spectra, when displayed with the hull-quotient removed, occurred on the absorption at 2156-2177 nm and 2227-2245 nm as a result of the mixture of clay minerals—kaolinite plus illite/smectite. Water absorptions occurred at 1912 nm and 1415 nm (Figure 3), the latter feature is also related to hydroxyl features in minerals. The depths and geometries of these features relate to the amounts of free versus bound water (interlayered with clay minerals), which can be used to distinguish pedolith and saprolith. In the VNIR regions, the crystal field absorption (CFA) of the iron oxides, hematite and goethite, was clearly definable by a broad 896 nm absorption and the charge transfer shoulder (CTS) as well as producing a charge transfer feature at 584 to 600 nm (Figure 4). Shifts in the wavelengths of these features are related primarily to the relative abundances of hematite and goethite, but also to the size fraction of the iron oxides, the abundance of opaque minerals and the substitution of Fe^{2+} and Al^{3+} (Cudahy & Ramanaidou 1997).

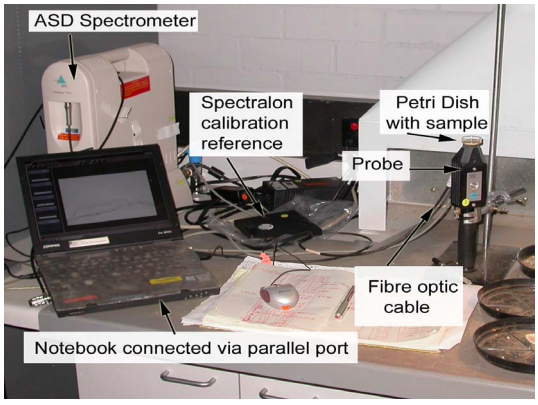

Figure 1: Laboratory setup of the ASD FieldSpec Pro FR using a High Intensity Contact Probe which houses the fibre optic cable and a 100 W halogen light source powered by the ASD. A notebook PC records the spectra and controls the instrument.

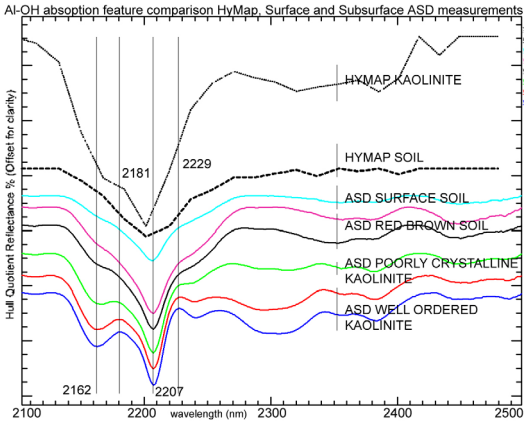

Figure 2: Aluminium hydroxide region (2200 nm) comparing HyMap™, surface and sub surface ASD measurements. The HyMap™ sensor possesses a lower spectral resolution resulting in apparent shifts in the absorption features.

The ASD FieldSpec measurements of the costean profiles exhibited a variation in spectral properties with depth. The upper samples displayed similar features to the surface traverse samples, which were termed the Post-European (PE) unit in reference to its interpreted deposition since pastoral settlement (Figure 5). In the areas close to the basement outcrop the PE unit was only seen in the upper-most sample. These areas were mapped as erosional rises (Brown *et al.* 2003), demonstrating that the slope angle of erosional rises closely corresponds with the thickness of material of the upper-most layers for these regolith-landform units. Aeolian and transported materials are less likely accumulate on rises due to erosional processes, which removes the material where deposits on the plains. Below the PE unit a discontinuous transitional layer appears to be a mixture of the upper-soil and the underlying red-brown (RB) pedal unit, which consists of aggregated, dark red- brown coloured hexagonal peds. The RB pedal unit can be differentiated from the PE unit by the deeper 1415 and 1912 nm water features as well as the stronger 2207 nm absorption. The CTS occurs at shorter wavelengths and the CFA is marginally deeper, related to increased development of goethite. A shift in the CTS was also seen between the crushed peds and unconsolidated sample material. The crushed samples displayed a shift in the CTS to longer wavelengths and a more rounded shoulder feature in the hull-quotient displayed reflectance spectra. This has been attributed to the differing grain sizes of the iron oxides in

aggregates and unconsolidated materials.

In the SWIR-2 region, features at 2165 nm, 2181 nm, 2206 nm and 2235 nm are related to kaolin and changes in its physicochemistry (Cudahy 1997). A relatively deep feature at 2181 nm is related to dickite, although in such regolith samples it is more related to dickite layers within kaolinite structure. That is, a type of kaolin disorder (Cudahy 1997). The 2229 nm shoulder for pure kaolinite is represented as an inflection in the right hand side of the peak and is related to cation substitution, typically Fe for Al (Cudahy 1997). In the RB and following units there is an increase in the depth of the 2162 nm absorption feature related to increasing kaolinite crystallinity (Cudahy 1997). There is also increasing development, and especially sharpness, of the 2229 nm feature within these same samples indicating that the lattice environment of the cations bonded to OH is becoming more ordered.

The unconformity between the top of weathered saprolite and the lower pedolith can be determined by the change in crystallinity of the mineral kaolinite, similar to other regolith environments in Australia (Cudahy *et al.* 1995, Cudahy 1997). The crystallinity of kaolinite can be determined by the relative depth of the 2162 nm absorption feature, with well-ordered kaolinite possessing a deeper absorption. Poorly-ordered kaolinite is generally indicative of *in situ* soils and transported materials. The weathered basement in the lower portion of the profiles displayed well-ordered kaolinite spectral signatures with deep 2206 nm, 2162 nm Al-OH absorptions and a 2229 nm shoulder. The spectra demonstrated a weak 1912 nm feature representing a lack of water, and a 1414/1399 nm doublet with a lack of iron oxide absorptions (Figure 3). The presence of goethite in the weathered saprolite was distinguishable from hematite by the deep broad 990 m crystal field absorption ($6A_1$->$4T_1$) and the presence of a 671 nm absorption related to the crystal field splitting energy ($6A_1$->$4T_2$) (Figure 4).

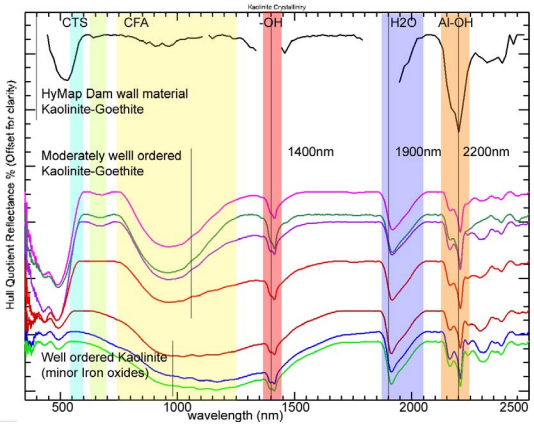

Figure 3: A spectral profile covering the VNIR and SWIR of kaolinite bearing materials demonstrating the main absorption features. Bands in the 1400 nm and 1900 nm wavelength regions have been omitted from the HyMap™ profile due to atmospheric effects.

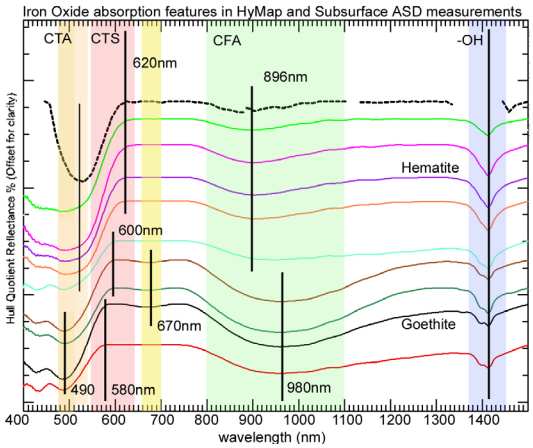

Figure 4: Iron oxide spectral properties comparison of HyMap™ and ASD results. The HyMap™ spectra, measuring the surface materials has similar features to ASD-hematite from samples in the upper profiles of the costeans. The lower profiles contain stronger goethite absorptions.

The AHSI was able to measure and map similar regolith minerals including the iron oxides and kaolin physicochemistries. For example, well-ordered kaolinite is identified in the HyMap™ spectra in pixels from saprolite exposed around dams (Figures 2 and 3). These dam walls were confirmed in the field to comprise weathered saprolite. ASD spectral analysis of the dam wall materials confirmed the occurrence of well-ordered kaolinite and goethite mineralogy. The presence of iron oxides was mapped, including the hematite-goethite ratio. The CFA and CTS were clearly defined in the HyMap™ imagery (Figure 4) with comparable spectral responses to the laboratory measurements. Regolith carbonate accumulations (RCAs) were found to be difficult to distinguish using spectral techniques in both the field spectrometer and the AHSI, consistent with other studies (Cudahy *et al.* 1992). The carbonate nodules from the profiles exhibited kaolinitic absorption features on the outer rind, but once crushed or dissected, displayed carbonate absorptions (Cudahy *et al.* 1992). When bulk samples were measured there was an absence or a minor carbonate absorption at 2300 nm. In general, mixed soil samples with a higher abundance of RCAs produced spectra of a higher reflectance, especially in the visible (Cudahy *et al.* 1992), unless the outer surfaces of the nodules were completely coated with fine soil material. From the HyMap™ imagery, a number of localities were identified and ground-truthed to show that rabbits had unearthered softer RCA material from depth. Note that some of

the spectra for the pixels in the AHSI identified as rabbit warrens displayed a significant 2300 nm absorption feature, related to carbonate absorption.

CONCLUSIONS

This study has shown that hyperspectral sensing, both remotely and in the field, can be used to measure and map regolith mineralogy, especially specific iron oxides and clays. A change in the absorption features in the 400-1500 nm region due to iron oxides can be used the mark the boundary between the upper soil layer (PE) and the underlying pedal RB soil unit. The boundary between the basement and the overlying soil layers can be identified by a change to well-ordered kaolinite crystallinity as well as a shift in the charge transfer shoulder of iron oxides at approximately 600 nm to shorter wavelengths in the saprolite. Goethite is present in the weathered saprolite at various depths, shown by a shift in the 896 nm CFA to longer wavelengths.

The spectral measurements demonstrated that the underlying saprolite displayed little resemblance to the overlying transported PE cover in the depositional plain. The surface measurements correlated with the corrected AHSI. Basement exposures had displayed different mineralogy to the weathered saprolite in the costeans and therefore appeared different to the hyperspectral imagery. Kaolinitic dam-wall material showed similar mineralogy of well-ordered kaolinite, hematite and goethite, representing weathered saprolite as found in the costeans.

Emphasis to date on regolith research has been on geochemistry with lesser attention given to regolith mineralogy. Mineralogy is a critical component for understanding and characterising regolith stratigraphy and related genetic processes. Hyperspectral sensing, via remote and proximal systems like HyMap^{TM} and PIMA/ASD, allows accurate mapping of regolith mineralogy. Regolith stratigraphy can be interpreted from these data given the right spectral-mineralogical regolith models. Further research is required to refine these models and understanding of the spectral properties of regolith materials.

REFERENCES

BROWN A., HILL S.M. & JAMES P. 2003. Detailed Regolith Mapping as a Tool for Refining the Interpretation of Geochemical Results at White Dam, Curnamona Craton, SA. *Broken Hill Exploration Initiative: Abstracts from the July 2003 conference*. Geoscience Australia **Record 2003/13**, 14-15.

COCKS T., JENSSEN A., STEWART A., WILSON I. & SHIELDS T. 1998. The HyMap^{TM} Airborne Hyperspectral Sensor: The System, Calibration and Performance. *1st EARSEL Workshop on Imaging Spectroscopy*, Zurich, October 1998.

CROWLEY J.K. 1986. Visible and near-infrared spectra of carbonate rocks: reflectance variations related to petrograpgraphic textue and impurities. *Journal of Geophysical Research* **89**, 6329-6340.

Cudahy T.J., Lintern M.J. & Gabell A.R. 1992. *Spectral properties of the soil overlying the site of the Bounty and North Bounty gold MINES, Forrestania region, Western Australia*. CSIRO, IMEC Division of Exploration Geoscience **Restricted Investigation Report No. 169R**, 60 pp.

CUDAHY T.J., GRAY D., PHILLIPS R.N. & WILDMAN J. 1995. *Pilot spectral study of the Bronzewing gold deposit, Western Australia*. CSIRO Exploration and Mining **Restricted Investigation Report 124R**, 99 pp.

CUDAHY T.J. & RAMANAIDOU E.R. 1997. Measurement of the hematite:goethite ratio using field visible and near-infrared spectrometry in channel iron deposits, Western Australia. *Australian Journal of Earth Sciences* **44**, 411-420.

CUDAHY T.J. 1997. *PIMA-II spectral characteristics of natural kaolins*. CSIRO Exploration and Mining **Report 420R**, 57 pp.

HUNT G.R., SALISBURY J.W. & LENHOFF C.J. 1971. *Visible and near infrared spectra of minerals and rocks: III. Oxides and hydroxides*. **Modern Geology 2**, 195-205.

LEWIS M., JOOSTE V. & DE GAPARIS A.A. 2001. Discrimination of Arid Vegetation with Airborne Multispectral Scanner Hyperspectral Imagery. *IEEE Transactions on Geoscience and Remote Sensing* **39(7)**, 1471-1479.

MCGEOUGH M. & ANDERSON J. 1998. *Discovery of the White Dam Au-Cu mineralisation*. Australian Geological Survey Organisation **Record 1998/25**, 69-71.

Acknowledgements: This research has been supported by a CRC LEME PhD scholarship and operating funds. The authors would like to acknowledge the following persons and organisations: MIM Exploration, Polymetals Pty Ltd., EXCO Pty Ltd. and Challenger Geological Services for access to data, core and the field area. The Station owners of Bulloo Creek and Tikalina for access to land and accommodation. The members of the Perth node CSIRO MMTG for their processing support and aid in interpretation of results. CRC LEME for use of the ASD Fieldspec instrument and financial support. PIRSA for data, geological background of the

Mingary mapsheet and remote sensing support. Special thanks to Steve Hill and Tom Cudahy for their thorough reviews.

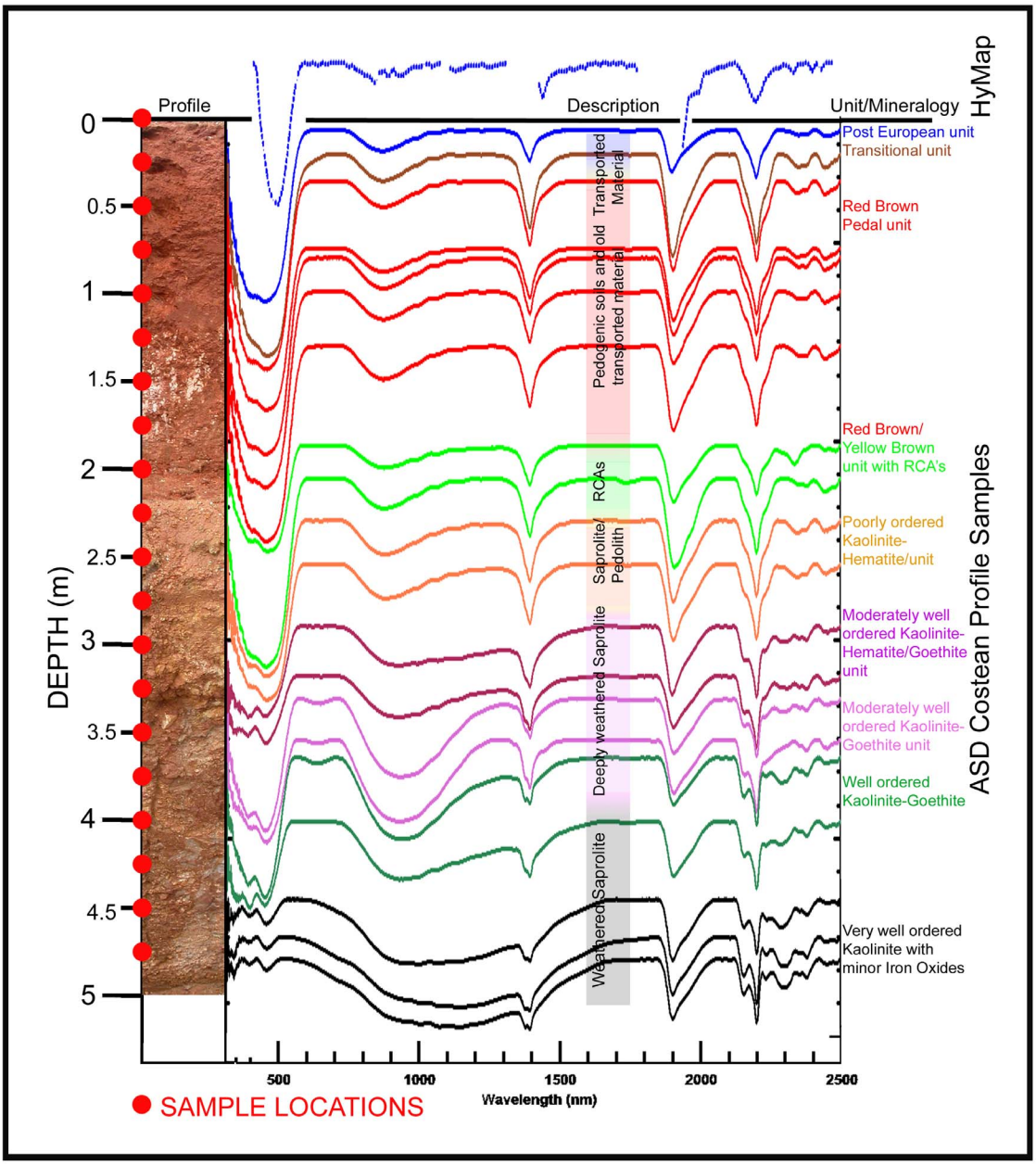

Figure 5: Complete spectral profile from a costean at White Dam with the associated HyMap^{TM} pixel response. The surface mineralogy consists of quartz, kaolinite, hematite and smectite which grades into soils and sediments with decreasing abundances of quartz and clays. At approximately 1-2 m above the saprolite there is an increase in regolith carbonate accumulations (RCA) with powdery nodules of 10-50 mm in diameter occurring. The poorly-ordered kaolinite absorption features become more distinctive as depth increases. In some localities the saprolite is capped by a thick layer of carbonate. The saprolite mineralogy consists of moderately well- to very well-ordered kaolinite, hematite and goethite.